

Novel Bis(ethylenedithio)tetrathiafulvalene-Based Organic Conductor with 1,1'-Ferrocenedisulfonate

Hiroki Akutsu,*† Ryo Ohnishi,† Jun-ich Yamada,† Shin'ichi Nakatsujii,† and Scott S. Turner‡

Graduate School of Material Science, University of Hyogo, 3-2-1 Kouto, Kamigori-cho, Ako-gun, Hyogo 678-1297, Japan, and Department of Chemistry, Warwick University, Gibbet Hill Road, Coventry CV4 7AL, U.K.

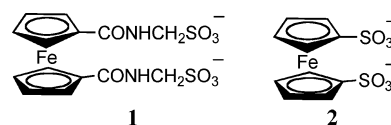
Received July 12, 2007

A new bis(ethylenedithio)tetrathiafulvalene (BEDT-TTF)-based salt with a ferrocenyl moiety, α''' -(BEDT-TTF)₄(Fe(C₅H₄SO₃)₂)·6H₂O, has been prepared. The ferrocenyl part of this salt is neutral and diamagnetic, but the magnetic susceptibility is well modeled by a Curie–Weiss law with $C = 0.142 \text{ emu}\cdot\text{K}\cdot\text{mol}^{-1}$ ($\approx 1/3$ of $s = 1/2$ spin). The spin is likely to be localized on the donor layer because of its unique charge disproportionation.

Charge-transfer salts of the electron donor molecule bis(ethylenedithio)tetrathiafulvalene (BEDT-TTF) exhibit a wide range of ground states, including metallic, superconducting, semiconducting, or insulating.^{1a} Typically, their structures consist of stacks of positively charged BEDT-TTF molecules that form layers that are interleaved by layers of counterions. The donor molecules pack in a variety of ways, leading to phases that are designated by the letters α , β , γ , κ , λ , etc.^{1,2} Evidently, the packing motifs play a crucial role in determining the electronic ground states. However, salts that have the same packing motif but different counteranions often have different ground states. In other words, additional structural subtlety can modify the ground states.^{1a,d} Recently, insulating states have been of interest to many researchers and various types of insulating states have been established,¹ such as charge-density wave, spin-density wave, Mott

insulator, charge-order, ferro- and antiferromagnetic order, and ferroelectric order.

Ferrocene is one of the most widely used functional materials. It is diamagnetic in the neutral state but has redox properties, and the monovalent cation is an $s = 1/2$ magnetic source.³ Because of its multifunctional properties, many researchers have introduced the ferrocenyl moiety into charge-transfer salts, although the resultant materials showed only semiconducting behavior.⁴ Recently, we prepared a sulfo derivative of the ferrocenyl moiety, Fe(Cp-CONHCH₂-SO₃⁻)₂ (**1**). The dianion gave two BEDT-TTF salts,⁵ one of which is the first metallic salt of this type in spite of the relatively large anion.^{5b} However, in the BEDT-TTF salt, the ferrocenyl moiety is neutral and diamagnetic probably because the oxidation potential of **1** is larger than that of BEDT-TTF because it has the electron-withdrawing group -CONHCH₂SO₃⁻. We have now prepared a BEDT-TTF salt with another ferrocenyl dianion, Fe(CpSO₃⁻)₂ (**2**). Here we report the structure and properties of this new salt.



The acidic dianion **2** was prepared according to the literature method.⁶ Metathesis with PPh₄Br gave orange

* To whom correspondence should be addressed. E-mail: akutsu@sci.u-hyogo.ac.jp.

† University of Hyogo.

‡ Warwick University.

- (1) (a) Williams, J. M.; Ferraro, J. R.; Thorn, R. J.; Carlson, K. D.; Geiser, U.; Wang, H. H.; Kini, A. M.; Whangbo, M.-H. *Organic Superconductors (including Fullerenes) Synthesis, Structure, Properties and Theory*; Prentice-Hall: New York, 1992. (b) Mori, T.; Kobayashi, A.; Sasaki, Y.; Kato, R.; Kobayashi, H. *Solid State Commun.* **1985**, *53*, 627. (c) Sasaki, T.; Lebed, A. G.; Fukase, T.; Toyota, N. *Phys. Rev. B* **1996**, *54*, 12969. (d) Miyagawa, K.; Kanoda, K.; Kawamoto, A. *Chem. Rev.* **2004**, *104*, 5635. (e) Takahashi, T.; Nogami, Y.; Yakushi, K. *J. Phys. Soc. Jpn.* **2006**, *75*, 051008. (f) Welp, U.; Fleshler, S.; Kwok, W. K.; Crabtree, G. W.; Carlson, K. D.; Wang, H. H.; Geiser, U.; Williams, J. M.; Hitsman, V. M. *Phys. Rev. Lett.* **1992**, *69*, 840. (g) Nad, F.; Monceau, P.; Yamamoto, H. M. *J. Phys.: Condens. Matter* **2006**, *18*, L509.
- (2) (a) Mori, T. *Bull. Chem. Soc. Jpn.* **1998**, *71*, 2059. (b) Mori, T. *Bull. Chem. Soc. Jpn.* **1999**, *72*, 179. (c) Mori, T. *Bull. Chem. Soc. Jpn.* **1998**, *72*, 2011.

- (3) (a) Miller, J. S.; Esptein, A. J.; Reiff, W. M. *Chem. Rev.* **1988**, *88*, 201. (b) Togni, A.; Hayashi, T., Eds. *Ferrocenes*; VCH Publishers: Weinheim, Germany, 1995.
- (4) (a) Ueno, Y.; Sano, H.; Okawara, M. *J. Chem. Soc., Chem. Commun.* **1980**, 28. (b) Moore, A. J.; Skabara, P. J.; Bryce, M. R.; Batsanov, A. S.; Howard, J. A. K.; Daley, S. T. A. K. *J. Chem. Soc., Chem. Commun.* **1993**, 417. (c) Wilkes, S. B.; Butler, I. R.; Underhill, A. E.; Kobayashi, A.; Kobayashi, H. *J. Chem. Soc., Chem. Commun.* **1994**, 53. (d) Wilkes, S. B.; Butler, I. R.; Underhill, A. E.; Hursthouse, M. B.; Hibbs, D. E.; Malik, K. M. A. *J. Chem. Soc., Dalton Trans.* **1995**, 897. (e) Moore, A. J.; Bryce, M. R.; Skabara, P. J.; Batsanov, A. S.; Goldenberg, M. L.; Howard, J. A. K. *J. Chem. Soc., Perkin Trans. 1* **1997**, 3443. (f) Lee, H.-J.; Noh, D.-Y.; Underhill, A. E.; Lee, C.-S. *J. Mater. Chem.* **1999**, *9*, 2359. (g) Iyoda, M.; Takano, T.; Otani, N.; Ugawa, K.; Yoshida, M.; Matsuyama, H.; Kuwatani, Y. *Chem. Lett.* **2001**, 1310.
- (5) (a) Furuta, K.; Akutsu, H.; Yamada, J.; Nakatsujii, S. *Chem. Lett.*, **2004**, 33, 1214. (b) Furuta, K.; Akutsu, H.; Yamada, J.; Nakatsujii, S.; Turner, S. S. *J. Mater. Chem.* **2006**, *16*, 1504.
- (6) Knox, G. R.; Pauson, P. L. *J. Chem. Soc.* **1958**, 692.

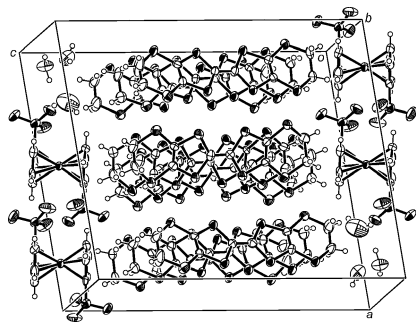


Figure 1. Crystal structure of **4**.

crystals of $(\text{PPh}_4)_2\mathbf{2}\cdot\text{H}_2\text{O}$ (**3**). X-ray diffraction data were collected with a Quantum CCD area detector on a Rigaku AFC-7R diffractometer, at room temperature.⁷ Two PPh_4 cations, two halves of **2**, and one water molecule are crystallographically independent. The Fe atoms are located on inversion centers. The distances between Fe and the Cp plane are 1.647 and 1.635 Å, respectively, which are similar to that of the unsubstituted ferrocene (1.654 Å).⁸ The oxidation potential of the dianion was determined by cyclic voltammetry.⁹ The E_1 value of **3** is 0.85 V, i.e., 0.30 V higher than that of BEDT-TTF ($E_1 = 0.55$ V) and 0.16 V higher than that of **1** ($E_1 = 0.69$ V).^{5a} This suggests that the ferrocenyl part would be neutral in the BEDT-TTF salts and that $-\text{SO}_3^-$ is a stronger electron-withdrawing group than $-\text{CONHCH}_2\text{SO}_3^-$.

Black plate crystals of α'' -(BEDT-TTF)₄(Fe(C₅H₄SO₃)₂)·6H₂O (**4**) were prepared by the controlled-current electrocrystallization method¹⁰ in a mixture of *o*-dichlorobenzene (28 mL) and acetonitrile (2 mL) with 20 mg of BEDT-TTF and 60 mg of **3**. Single-crystal X-ray diffraction data of **4** were recorded using a Quantum CCD area detector on a Rigaku AFC-7R diffractometer at room temperature.¹¹ The crystal structure (Figure 1) has an asymmetric unit with six BEDT-TTF molecules (A–F), one and a half of **2**, and nine water molecules. The crystal lattice consists of alternating layers of the donor and anion/water layers. The donor layers are in an α'' -type packing motif¹² (Figure 2a), and the anion layers have a 2-D hydrogen-bonded network of $-\text{SO}_3^-$ and H₂O (Figure 2b).

The α'' -type donor layer has two types of overlap modes along the *a* (side-by-side) direction; one is an α -type motif

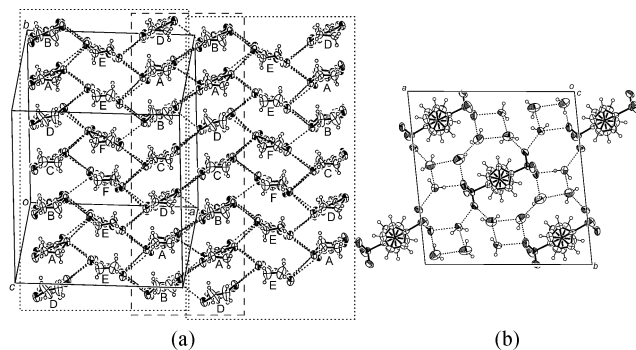


Figure 2. (a) α'' -type packing motif of the donor layer of **4**. Dashed lines indicate short S···S distances (<3.7 Å). (b) 2-D hydrogen-bonded network of the anion/water layer of **4**. Dashed lines indicate hydrogen bonds ($\text{O}\cdots\text{O} < 3.05$ Å).

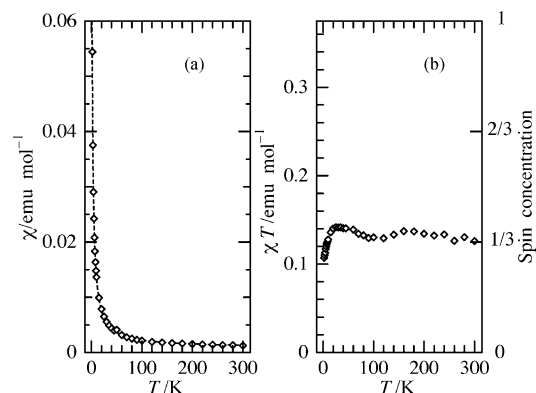


Figure 3. Temperature-dependent magnetic susceptibility of a powder sample of **4**. (a) χ vs T plots of **4**. The dashed line is calculated on the basis of a Curie–Weiss expression. (b) χT vs T plots of **4**.

(bound by the dotted line in Figure 2a), and the other is a β'' -type motif (bound by dashes in Figure 2a). The three crystallographically independent Fe-to-ring-center distances of 1.647, 1.652, and 1.646 Å are not close to that in a ferrocene cation (1.705 Å) but are close to those in **3**, indicating that the ferrocenyl part is in the neutral state. This is consistent with the cyclic voltammetry data above. Therefore, each BEDT-TTF molecule in **4** has a formal charge of +0.5.

The electrical resistivity, as measured down to 100 K, is semiconductive with $\rho_{\text{RT}} = 13 \Omega\cdot\text{cm}$ and $E_a = 0.22$ eV. The room-temperature electrical resistivity and the activation energy are higher than those of other BEDT-TTF^{0.5+} salts, suggesting the formation of a density wave or a charge ordering even at room temperature. The magnetic susceptibility of a polycrystalline sample from 2 to 300 K was measured using a Quantum Design MPMS-5S SQUID magnetometer (Figure 3). The temperature-dependent magnetic susceptibility is explained by the Curie–Weiss model with $C = 0.142 \text{ emu}\cdot\text{K}\cdot\text{mol}^{-1}$, $\theta = -1.09$ K, and $a = 8.4 \times 10^{-4} \text{ emu}\cdot\text{mol}^{-1}$, where C is the Curie constant, θ is the Weiss temperature, and a is a temperature-independent paramagnetic term. The result clearly indicates that there is a localized spin. Because the ferrocenyl moiety is diamagnetic, the spins must be located on the donor layer. The C value is 38% of that of the $s = 1/2$ spin ($0.375 \text{ emu}\cdot\text{K}\cdot\text{mol}^{-1}$). It can be considered that two of six electron holes (33%) in the unit cell are localized.

(7) Crystal data for **2**: C₅₈H₅₀FeO₇P₂S₂, $M = 1040.94$, triclinic, space group $P\bar{1}$, $a = 10.6112(4)$ Å, $b = 15.3656(5)$ Å, $c = 16.6603(12)$ Å, $\alpha = 67.156(2)^\circ$, $\beta = 81.1619(6)^\circ$, $\gamma = 83.4457(8)^\circ$, $V = 2469.2(2)$ Å³, $Z = 2$, $D_c = 1.400 \text{ g}\cdot\text{cm}^{-3}$, $F(000) = 1084$, $\mu(\text{Mo K}\alpha) = 0.5098 \text{ mm}^{-1}$, $T = 293$ K, 10 682 unique reflections [$R(\text{int}) 0.032$], $R(\text{on } F) = 0.063$, $wR(\text{on } F) = 0.061$ [$I > 2\sigma(I)$].

(8) Almninggen, A.; Haaland, A.; Samdal, S. *J. Organomet. Chem.* **1978**, *149*, 219.

(9) Voltage versus saturated calomel electrode in PhCN with 0.1 M Bu₄NClO₄, Pt electrode, at room temperature, under nitrogen (scan rate = 50 mV·s⁻¹).

(10) Anzai, H.; Delrieu, J. M.; Takahashi, S.; Nakatsuji, S.; Yamada, J. *J. Cryst. Growth* **1995**, *154*, 145.

(11) Crystal data for **3**: C₅₀H₅₂FeO₁₂S₃, $M = 1990.84$, triclinic, space group $P\bar{1}$, $a = 16.7469(10)$ Å, $b = 17.4917(16)$ Å, $c = 19.7235(17)$ Å, $\alpha = 100.1831(18)^\circ$, $\beta = 99.3893(6)^\circ$, $\gamma = 94.1645(8)^\circ$, $V = 5579.7(8)$ Å³, $Z = 3$, $D_c = 1.777 \text{ g}\cdot\text{cm}^{-3}$, $F(000) = 3054$, $\mu(\text{Mo K}\alpha) = 1.2131 \text{ mm}^{-1}$, $T = 295$ K, 23 577 unique reflections [$R(\text{int}) 0.080$], $R(\text{on } F) = 0.078$, $wR(\text{on } F) = 0.066$ [$I > 3\sigma(I)$].

(12) Shibaeva, R. P.; Yagubskii, E. B. *Chem. Rev.* **2004**, *104*, 5347.

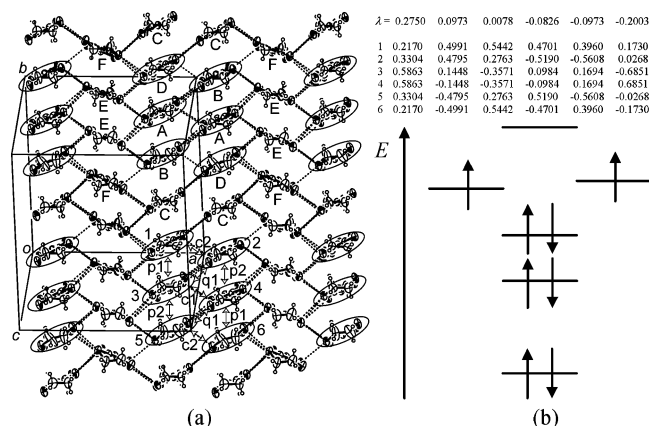


Figure 4. (a) Packing arrangement of BEDT-TTF. Circled donors have an approximately 0.3 Å longer central C=C bond length than those of the others. (b) Table of eigenvalues (λ of $\epsilon = \alpha + \lambda\beta$) and eigenvectors (factors for molecular orbitals) and a pictorial representation of the energy diagram for the hexamer calculated by a simple Hückel molecular orbital method.

The central C=C bond lengths of six independent BEDT-TTF molecules A–F are 1.388(11), 1.380(12), 1.354(11), 1.380(12), 1.357(12), and 1.360(11) Å, respectively. The lengths are divided into two categories: long (1.380–1.388 Å for A, B, and D) and short (1.354–1.360 Å for C, E, and F). Usually, molecules having longer C=C bond lengths have higher charges. Figure 4a again shows the donor layer, in which A, B, and D, carrying the higher charges, are circled. Interestingly, the circled molecules form hexamers that are surrounded and separated by the other molecules. This implies that the spin seems to be localized on the hexamer.

We have estimated the charge on each BEDT-TTF molecule using bond lengths,¹³ which gives charges for A–F of +0.79, +0.72, +0.37, +0.70, +0.47, and +0.50, respectively. Therefore, each hexamer ($A_2B_2D_2$) has a charge of +4.42, and the other six molecules ($C_2E_2F_2$) have a charge of +2.68. The charges, normalized by the total number of the holes in the unit cell, are +3.75 for the hexamer and +2.25 for the others. So, we can roughly say that the hexamer has four holes and the other molecules have two holes. The intrahexamer overlap integrals between donors in the hexamer were calculated.¹⁴ The values ($\times 10^{-3}$) for p1, p2, q1, c1, and c2 (Figure 4a) are -5.39, +4.71, -7.64, +18.55, and +8.50, respectively.

We have also calculated an energy diagram for the hexamer using simple Hückel molecular orbital theory with

two assumptions: (1) The hexamer is regarded as six conjugated atoms that have nine bonds (see Figure 4a), and (2) the resonance integral β is proportional to the calculated overlap integrals; thus, the resonance integral $\beta(t) = 10.0|t|$, where t is the calculated overlap integral (p1, p2, q1, c1, or c2). The secular equation is as follows:

$$\begin{vmatrix} -\lambda & \beta(c2) & \beta(p1) & 0 & 0 & 0 \\ \beta(c2) & -\lambda & \beta(q1) & \beta(p2) & 0 & 0 \\ \beta(p1) & \beta(q1) & -\lambda & \beta(c1) & \beta(p2) & 0 \\ 0 & \beta(p2) & \beta(c1) & -\lambda & \beta(q1) & \beta(p1) \\ 0 & 0 & \beta(p2) & \beta(q1) & -\lambda & \beta(c2) \\ 0 & 0 & 0 & \beta(p1) & \beta(c2) & -\lambda \end{vmatrix} = 0$$

where ϵ is the eigenvalue, α is the Coulomb integral, and $\lambda = (\epsilon - \alpha)/\beta$. The result is shown in Figure 4b. The second-highest two orbitals are practically degenerated, and most of the electron densities for both orbitals are localized on the four outer molecules (1, 2, 5, and 6 in Figure 4a) like a molecular orbital with antibonding character. Because the hexamer has four holes (eight electrons), as shown in Figure 4b, the doubly degenerate orbitals, which now become the highest occupied molecular orbitals, have two electrons. Thus, there are two spins in the unit cell. This simple calculation is consistent with the magnetic data, indicating that approximately one-third of the valence electrons are localized. In addition, a relatively large temperature-independent magnetic susceptibility of $8.4 \times 10^{-4} \text{ emu}\cdot\text{mol}^{-1}$ is observed, which seems to be Pauli paramagnetism. This suggests that the holes external to each are delocalized over the donor layer with strong electron–electron correlations.

In conclusion, the electrocrystallization of BEDT-TTF with $\text{PPh}_4\cdot\text{Fe}(\text{CpSO}_3)_2$ gave $\alpha'''\text{-(BEDT-TTF)}_4(\text{Fe}(\text{CpSO}_3)_2)\cdot 6\text{H}_2\text{O}$. The donor molecules form a 2-D conducting sheet, separated by anions and water molecules. The ferrocenyl part in the salt is neutral, but the magnetic susceptibility can be fitted by a Curie–Weiss model with $C = 0.142 \text{ emu}\cdot\text{K}\cdot\text{mol}^{-1}$, $\theta = -1.09 \text{ K}$, and $a = 8.4 \times 10^{-4} \text{ emu}\cdot\text{mol}^{-1}$. The results indicate that approximately one-third of the valence electrons are localized on the donor layer because of a unique charge disproportionation, and the remaining electrons are delocalized with strong electron–electron correlations.

Acknowledgment. This work was supported by a foundation of the University of Hyogo (2006).

Supporting Information Available: Crystallographic CIF files for **3** and **4**. This material is available free of charge via the Internet at <http://pubs.acs.org>.

IC701392Z

(13) Guionneau, P.; Kepert, C. J.; Bravic, G.; Chasseau, D.; Truter, M. R.; Kurmoo, M.; Day, P. *Synth. Met.* **1997**, *86*, 1973.

(14) Mori, T. Energy band calculation software package. See <http://www.op.titech.ac.jp/lab/mori/lib/program.html>.